Journal of Stress Analysis
Vol. 1, No. 2, Autumn – Winter 2016-17
Bu-Ali Sina University

Failure Mechanism and Ultimate Strength of Friction Stir Spot Welded Al-5052 Joints under Tensile-shear Loading

M.H. Salimi, M. Assadollahi, S. Nakhodchi*
Mechanical Engineering Department, K.N. Toosi University of Technology, Tehran, Iran.

Article info

Article history:
Received 2017.01.07
Received in revised form
2017.02.15
Accepted 2017.03.06

Keywords:
FSSW
failure mechanism
analysis
tensile-shear load

Abstract

In this paper failure mechanism of a joint which was welded by friction stir spot welding method was studied. The 5052 aluminum joint was loaded under tensile-shear condition.To find out failure mechanism, several tests were conducted such as: strain-stress, macrography, and Vickers hardness. Results of strain-stress test state the stages of failure and crack initiation and propagation. Macrography analysis was done in several stages with different penetration depths. It was shown that the material flow, the critical surface of the coupon, and the determined zones were more possible to generate crack. Finally, by using Vickers hardness test, the susceptible zones to crack generation and propagation can be specified.

1. Introduction

Recently, a new joining technique called friction stir spot welding (FSSW) or friction spot joining (FSJ) has been developed [1-3]. The advantages of FSSW are: solid-state process, ease of handling, dissimilar welding, low distortion, good mechanical properties, and little waste. Hence, itisused to weld light weight materials for several reasons such as high performance and energy and cost saving of machines and structures. First time it was proposed by the Welding Institute (TWI) of UK in 1991, and then it was spread by Mazda Corporation of Japan [4]. The FSSW process has three stages, i.e., plunging, stirring and retracting as shown in Fig. 1. First the tool started spinning with high rotational speed, and then the tool was slowly plunged into two overlapping sheets at a single location. Then a certain dwelling time was necessary to mix materials of sheets. It takes usually about 2 to 5 seconds. Finally, a solid-state bond was made between the interface of the upper and lower sheets and the tool was drawn out [5].

Previously, tool's material in FSSW was a limiting parameter such that the joining process was limited to aluminum alloys. However, with the development of new tool materials, this process can be applied to weld steels [5]. This problem was solved and several materials were welded by FSSW. Many studies have been conducted on microstructures, mechanical properties, and fatigue behavior of FSSW of several materials [6-21].

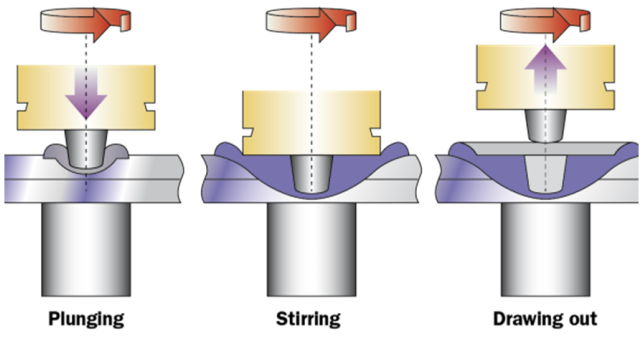

Fig. 1. FSSW procedure [6].

The strength of the welding materialisa critical point, and it is affected by several factors such as tool

*Corresponding author: S. Nakhodchi (Assistant professor)
E-mail address: snakhodchi@kntu.ac.ir

geometry and process parameters. To control heat generation and material flow, selecting parameters of toolsare extremely important. Generally, these parametersare shoulder diameter, shape, pin shape, length, diameter and feature [9]. Currently, one of the most conventional designsis a concave tool shoulder whereas thereare some flat tool shoulder designs [10]. Arul et al. reported that concave shoulder tool produced higher joint strength than the flat shoulder tool during FSSW of aluminum [22]. Badarinarayan also conducted a research to compare concave and convex tool profiles; it was presented that concave profile shoulder exhibited higher weld strength than those using convex or flat shoulder [23]. FSSW with galvanized steel joints were fabricated by Baek. As a result, it was clear that there was no mechanically mixed layer between the top and bottom plates at the weld nugget due to the limited tool penetration and the lower pin height of the welding tool than the steel plate thickness [24]. Baek studied low-carbon steel plates with lap configuration which were joined by FSSW; it was found that the tool penetration depth exerted a strong effect on failure mode of joining samples [25]. Some of the previous researches stated that low rotational speed caused high strength of welds [26-28]. However, Hunt et al. noticed that increasing the tool rotational speed increased the joint strength [29]. Tran et al. discovered that the strength had direct relationship with duration time in aluminum alloys [30]. Sato et al. reported that initial oxide layer on the buttsurface during FSSW hadoften deleterious effects on the mechanical properties of the weld [31].

In this paper the goalis to determine failure mechanism and ultimate strength of joints that were welded by FSSW witha tensile-shear stressapplied to them. In section 2, material, geometry of coupon, tool specification and FSSW procedure were explained. Then a tensile-shear load was applied to joints. Afterwards, the results of tensile-shear test and macrography test were reported. The failure mechanism of joints was determined by using results of tests.

2. Material and Experimental Procedure

The material used was aluminum AA 5052-H36, with thickness of 2mm. This alloy is categorized in the Al-Mg alloys groups. The chemical composition was specified by Spark Emission Spectrometer and the mechanical properties were tested by the stress-strain test. These results are listed in Table 1 and Table 2 respectively. This alloy has good corrosion resistance and weld ability so that it is a common material in aerospace, automotive, and marine industries.

Table 1
Chemical composition of 5052 Al alloy.

Element	Al	Mg	Fe	Cr	Sc	Others
Weight percentage	Rest	2.5	0.4	0.25	0.25	0.45

Table 2
Mechanical properties of 5052 Al alloy.

Mechanical property	Unit
Yield stress	241MPa
Ultimate stress	276MPa
Elongation	8%
Melt temprature	622°C

A tool was made with a shoulder diameter of 13mm and concave profiles. Its geometry and welded nuggetsare shown in Fig. 2 and Fig. 3 respectively. The pin was conical unthreaded, with 2.75mm in length and 15 degree in apex angle. The angle of chamfer within the shoulder end surface was 3 degree. A plunge speed of 12mm/min and a dwell time of 5 second were adopted in this study. The tool rotation speed was fixed to 2,500rpm. The tools were made of hot-work tool steel H13 with commercial name 1.2344 and all of them were hard worked until 50 HRC.

All specimens in this project were lap joint and the dimensions of the sheets were 200×30mm. This size was based on an industrial part and was selected in order to eliminate the effects of tension concentration. The width of specimens was about 3 times greater than the effective area of the nuggets. The distances between the nugget's center and the sheet's edge and between two centers were designed 15mm and 30mm respectively to prevent the stress concentration. This geometry is shown in Fig. 4 and the other specimens were welded based on this geometry.

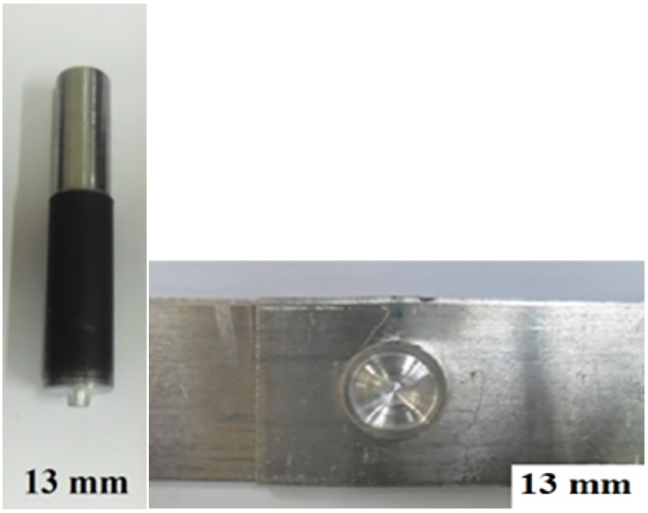

Fig. 2. The tool (left) and nugget (right).

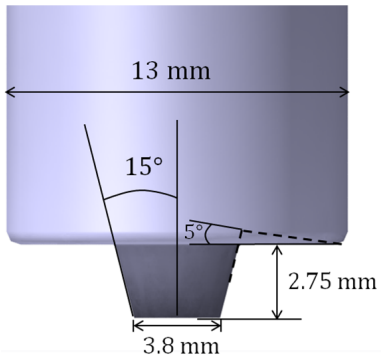

Fig. 3. Geometry of the tool.

Totally, eight specimens based on this geometry were produced. To study the effects of the tool penetration, six specimens were used.

To study micro structures of samples, an optical microscope was used. After failure the profiles of the specimens were cut, polished, and mounted. To increase resolution of the surfaces, alkaline etchant solution for aluminum series 5 was used. The images were captured with a 25X and a 50X zoom. The hardness at the profile was specified by the Vickers hardness method. The used apparatus was the Microhardness Tester.

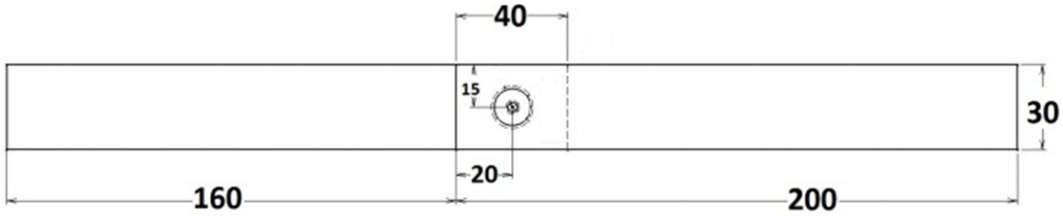

Fig. 4. Geometry of specimens and coupon.

The joints was welded by FP4ME CNC milling machine and the tensile-shear tests were done in room temperature and a loading speed of 1mm/min by Shijin-Class A testing machine (Fig. 5). To align forces in the tensile test, a square sheet with a 30mm side was joined to the specimens with metal adhesive. The tests were replicated 3 times in each stage and finally the results were averaged. It should be noted that all of tests were done based on the ISO/DIS 18785-4 standard.

3. Results and Discussion

3.1. Macrostructure Failure Mechanism

The diagram of force-displacement of a single weld that fractured in a button-pullout modeis shown in Fig. 6. The applied tensile-shear force (TSF) was slightly over 900 N. Since fracture initiates at the load increment immediately following the TSF, the TSF may also be designated as the fracture initiation force. The endpoint of displacement, ΔL, was about 6mm. At this point, deformation became localized around the joint and catastrophic failure followed.

The diagram in Fig. 6 was divided into six sections by vertical lines in the figure. In section #1, the force was not changed and it can be considered constant, thus the displacement wasnot typically very large. After that the grips were tightened by preloading, this section was ultimately eliminated. There was not a significant deviation in diagram, because resulting difference was small enough.

It can be seen a proportional relationship between force and displacement in section #2, so the coupons were in elastic deformation condition.

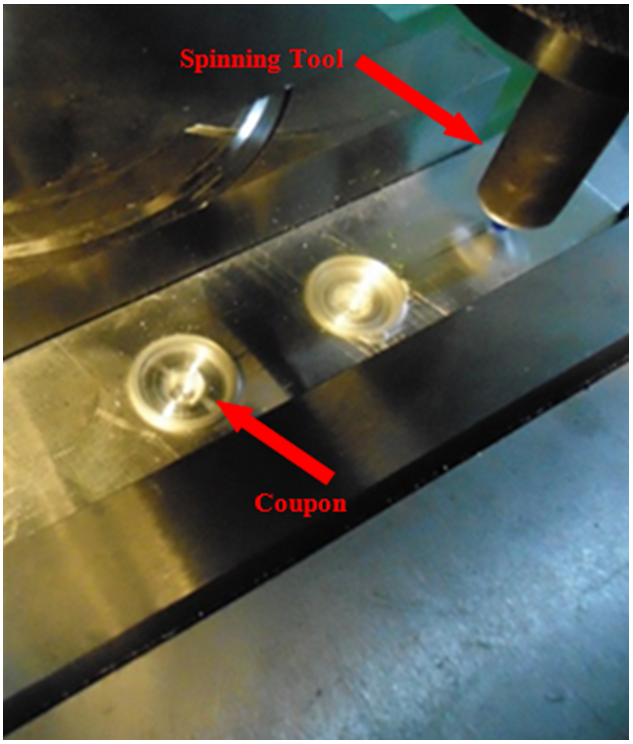

Fig. 5. Welding procedure.

There was proportional relationship in section #3 such as section #2 but its slope diminished slightly. If loadis eliminated, approximately the coupons return to their initial dimensions. It can be inferred that prevailing deformation conditions were elastic but there was a small degree of plastic deformation. At the inflection point between #2 and #3 the coupons were bent. This out-of-plane deformation occurred due to

the bending moment through out the ungripped section of the coupon.

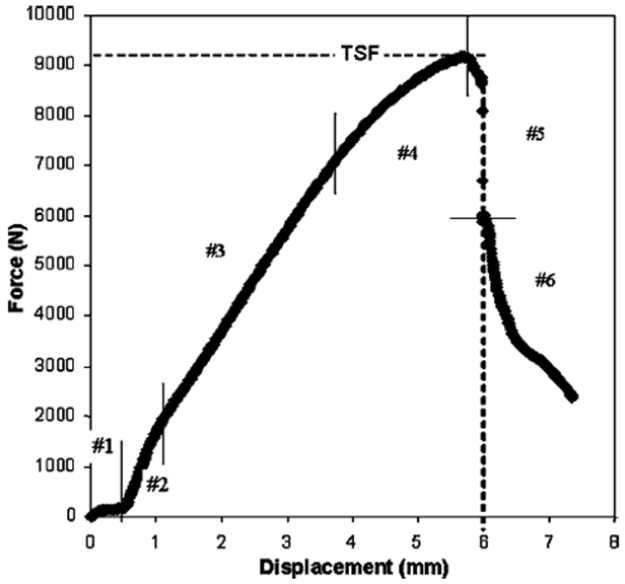

Fig. 6. The result of strain-stress test.

In section #4, the force reaches its maximum value, i.e., the TSF. The bending moment controlled the force response largely in this section. When it reached the TSF, the stress became localized in the joint region to the extent that fracture initiated, so with load increment, the downward trend was initiated. It can be seen in section #5. The force immediately drops to zero, so fracture can be characterized as interfacial.

When fracture started, crack propagation throughout the entire thickness occurred. This event occurred by rotation of the coupon and it was related to section #6. The residual force and displacement cause fracture propagation into the base metal, when the weld is fully rotated.

3.2. Microstructure Failure Mechanism

To evaluate the surface of weld, macrographic analysis was done. The upper surfaces of the joints obtained from different penetration depthare shown in Fig. 7. It can be seen easily that how the lowest and highest values of depth lead respectively to a poor material mixing and to a remarkable coupon diameter.

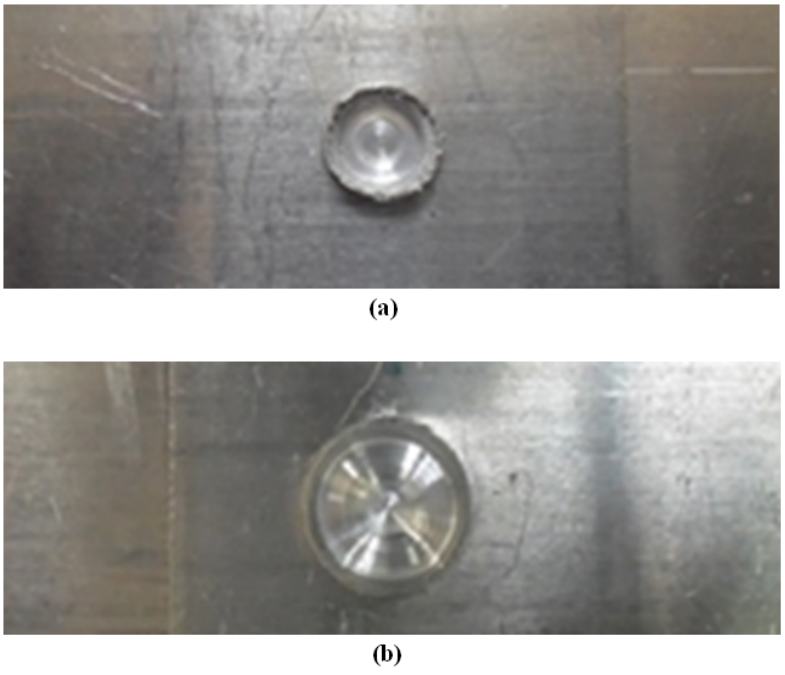

Fig. 7. Upper surface of the joints obtained by different penetration depth, initial penetration (a), finalpenetration (b).

The sections of the joints, after alkaline etching, are shown in Fig. 8. Indeed in Fig. 8a penetration of tool was in initial stage and just pin was in contact with surfaces. In Fig. 8b plunging of tool was completed and both pin and shoulder were plunged in the nugget. The effective thickness and the hook were two important factors in this analysis. The distance between the shoulder and the position of partial metallurgical bond was the Effective top sheet thickness (Teff). The distance between the interface of the two sheets and the end point of Teff was Hook height (Hh). Beside these two definitions, another area can be specified as stir zone (SZ). The stir zone was an area which the materials were flowed and stirred by rotation of tool. The width of the stir zone can be estimated by calculation of the distance between the edge of the key hole and

the widest region of the stir zone. Width of stir zone has significant effect on the UTSF of joints.

Two different joints morphology was observed in this figure: for low penetration depth, the joint line was almost straight. For high penetration depth, the joint line was curved and the hook was clearly visible. Changing the joint interface to a curved line was caused by the subjected severe plastic deformation during friction stirring. The crack was initiated from unmixed region and reached the pinhole by propagating the stir zone.

Penetration and rotation of tool generated a material flow which the material from the bottom sheet was extruded and pushed upward closer to the pinhole. It can be observed that area of SZ in high penetration was more than the low penetration, because shoulder of tool can stir more materials than pin. So when penetration increased and shoulder's contact increased gradually, the SZ became wider. Besides this, an unmixed region in Fig. 8a indicates that the joint bonding was initiated, but not completed in full due to a low penetration depth.In Fig. 8b the joints showed better tensile-shear failure loads compared to their counter part due to the extrusion of more metal towards the shoulder region.

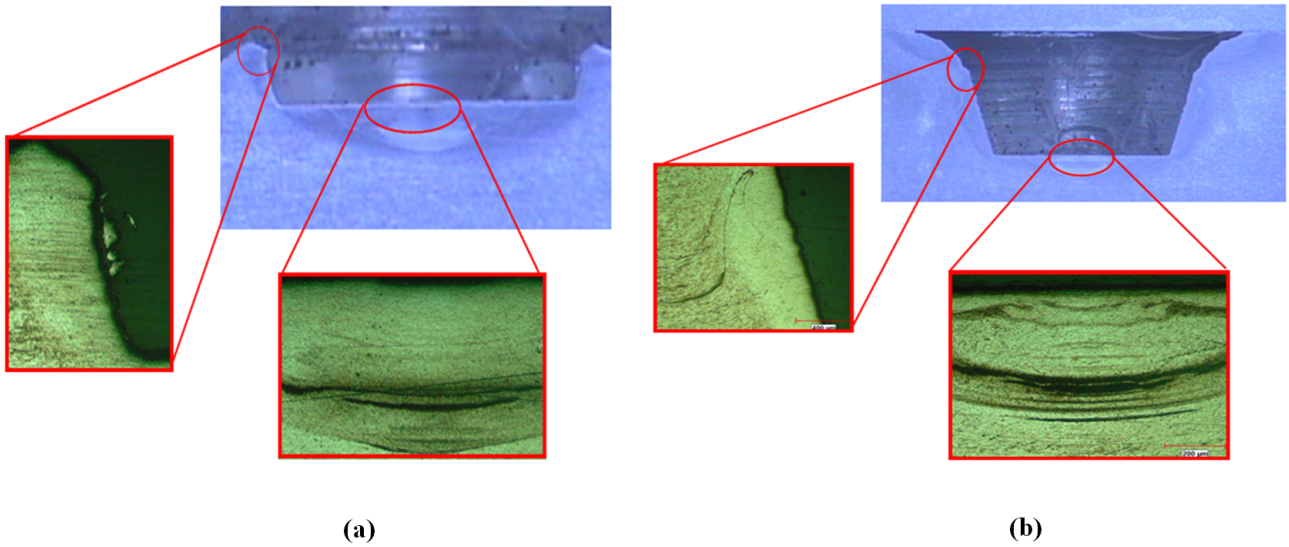

Fig. 8. Macrostructure of joints, (a) low penetration, (b) high penetration.

3.3. Hardness

Fig. 9 shows the Vickers hardness profiles in the mid-thickness of the upper and lower sheets respectively. According to this profile, the distribution of Vickers hardness was symmetric and had a W shape. In general, the Vickers hardness in both of the upper and the lower sheets decreased as closer to center. The hardness of the base material (BM) was about 75 HV. The hardness of the welds was lower than that of the base metal. In location of HAZ, Vickers hardness decreased gradually, reaching the minimum value of 47 HV around the HAZ and TMAZ. The harness of this zone was equivalent to 78% of the base material hardness. The hardness increased dramatically in TMAZ and SZ. The frictional heating affect the HAZ and the grains in the HAZ get coarser than that of the BM;so coursing in grain size causes the reduction of Vickers hardness in HAZ. The microstructure in TMAZ experiences both moderate frictional heating and deformation and was characterized by ahighly deformed structure. Intense plastic deformation and high temperatures induce dynamic recrystallization the SZ.

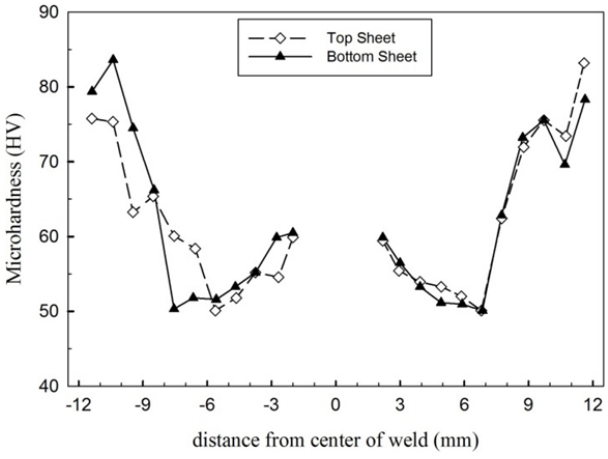

Fig. 9. Hardness of weld profile by Vickers test.

4. Conclusions

In this paper failure mechanism of aluminum 5052 jointwhich was welded by friction stir spot welding (FSSW) method under tensile-shear loading was studied. The

force-displacement diagram had five parts which determined the behavior of these joints. After peak point of diagram, the curvature dropped immediately, so mechanism of failure was pull-shear out mechanism. Although the specimens were under the tensile stresses, but the couponswere yielded by shear stresses, because the coupon rotated under the tensile force. So the welds must be designed based on the shear stresses.As the depth penetration increased, more materials were extruded under the weld zone. It was seen that the shoulder of tool can stir more materials than pin. Thus the wide of stir zone increased and because of it, the UTSF increased. The captured figures from macrography test proved this claim. Profile of Vickers hardness test stated that the hardness of the base metal was more than the other zone. At the HAZ, hardness was the minimum value. It can be inferred that the possibility of propagation of cracks in the base metal were more than the HAZ.

References

[1] D. Kim, Resistance spot welding of aluminum alloy sheet 5J32 using SCR type and inverter type power supplie, Mat. Sci. Eng., 38 (2009) 55-60.

[2] L. Han, M. Thornton, M. Shergold, A comparison of the mechanical behaviour of self-piercing riveted and resistance spot welded aluminium sheets for the automotive industry, Mater. Design., 31 (2010) 1457-1467.

[3] A. Gean, Static and fatigue behavior of spot-welded 5182-0 aluminum alloy sheet, Weld. J., 78 (1999) 80-88.

[4] Y. Tozaki, Y. Uematsu, K. Tokaji, Effect of tool geometry on microstructure and static strength in friction stir spot welded aluminium alloys, Int. J. Mach. Tool. Manu., 47 (2007) 2230-2236.

[5] Y. Uematsu, K. Tokaji, Comparison of fatigue behaviour between resistance spot and friction stir spot welded aluminium alloy sheets, Sci. Technol. Weld. Joi., 14 (2009) 62-71.

[6] D. Choi, Formation of intermetallic compounds in Al and Mg alloy interface during friction stir spot welding, Intermetallics, 19 (2011) 125-130.

[7] A. Gerlich, P. Su, T. North, Tool penetration during friction stir spot welding of Al and Mg alloys, J. Mater. Sci., 40 (2005) 6473-6481.

[8] K. Muci-Küchler, S. Kalagara, W.J. Arbegast, Simulation of a refill friction stir spot welding process using a fully coupled thermo-mechanical FEM model. J. Manuf. Sci., 132 (2010) 145-155.

[9] M. Bilici, A.I. Ykler, Influence of tool geometry and process parameters on macrostructure and static strength in friction stir spot welded polyethylene sheets. Mater. Design., 33 (2012) 145-152.

[10] M. Merzoug, Parametric studies of the process of friction spot stir welding of aluminium 6060-T5 alloys. Mater. Design., 31 (2010) 3023-3028.

[11] Y. Yin, A. Ikuta, T. North, Microstructural features and mechanical properties of AM60 and AZ31 friction stir spot welds. Mater. Design., 31 (2010) 4764-4776.

[12] S. Thoppul, R.F. Gibson, Mechanical characterization of spot friction stir welded joints in aluminum alloys by combined experimental/numerical approaches: Part I: Micromechanical studies. Mater. Charact., 60 (2011) 1342-1351.

[13] M. Kurtulmus, Friction stir spot welding parameters for polypropylene sheets. Sci. Res. Essays., 7 (2012) 947-956.

[14] S. Jambhale, S. Kumar, S. Kumar, Effect of process parameters & tool geometries on properties of friction stir spot welds: a review, J. Eng. Sci., 3 (2015) 6-11.

[15] S. Siddharth, T. Senthilkumar, Study of Friction Stir Spot Welding Process and its Parameters for Increasing Strength of Dissimilar Joints, JSA, 5 (2011) 144-150

[16] W. Yuan, Friction stir spot welding of aluminum alloys, JSA, 1 (2008) 10-18.

[17] D. Klobčar, Parametric study of friction stir spot welding of aluminium alloy 5754. Metalurgija, 53 (2014) 21-24.

[18] C. Jonckheere, Fracture and mechanical properties of friction stir spot welds in 6063-T6 aluminum alloy, Int. J. Adv. Manuf. Tech., 62 (2012) 569-575.

[19] G. Buffa, L. Fratini, M. Piacentini, On the influence of tool path in friction stir spot welding of aluminum alloys. J. Mater. Process. Tech., 208 (2008) 309-317.

[20] Q. Yang, Material flow during friction stir spot welding. Mater. Sci. Eng., 527 (2010) 4389-4398.

[21] A. Malafaia, Fatigue behavior of friction stir spot welding and riveted joints in an Al alloy, Proc. Eng., 2 (2010) 1815-1821.

[22] S. Arul, Experimental study of joint performance in spot friction welding of 6111-T4 aluminium alloy, Sci. Technol. Weld. Joi., 13 (2008) 629-637.

[23] H. Badarinarayan, Effect of tool geometry on hook formation and static strength of friction stir spot welded aluminum 5754-O sheets, Int. J. Mach. Tool. Manu., 49 (2009) 814-823.

[24] S. Baek, Microstructure and mechanical properties of friction stir spot welded galvanized steel, Mater. T., 51 (2010) 1044-1050.

[25] S. Baek, Structureproperties relations in friction stir spot welded low carbon steel sheets for light weight automobile body, Mater. T., 51 (2010) 399-403.

[26] T. Freeney, S. Sharma, R. Mishra, Effect of welding parameters on properties of 5052 Al friction stir spot welds, SAE Technical Paper, 150 (2008) 171-191.

[27] Z. Zhang, Effect of welding parameters on microstructure and mechanical properties of friction stir spot welded 5052 aluminum alloy, Mater. Design., 32 (2011) 4461-4470.

[28] Y. Tozaki, Y. Uematsu, K. Yokaji. Effect of welding condition on tensile strength of dissimilar friction stir spot welds between different aluminum alloys. in 6th International Symposium on Friction Stir Welding (ISFSW6), Montreal, QC, Canada, Oct. 2006.

[29] F. Hunt, H. Badarinarayan, K. Okamoto, Design of Experiments for Friction Stir Stitch Welding of Aluminum Alloy 6022-T4-Friction Stir Welding of Aluminum for Automotive Applications, SAE Technical Paper, 142 (2006) 84-93.

[30] V. Tran, J. Pan, T. Pan, Effects of processing time on strengths and failure modes of dissimilar spot friction welds between aluminum 5754-O and 7075-T6 sheets. J. Mater. Process. Tech., 209 (2009) 3724-3739.

[31] S. Sato, Characteristics of the kissing-bond in friction stir welded Al alloy 1050. Mat. Sci. Eng., 405 (2005) 333-338.